



ELSEVIER

Available online at www.sciencedirect.com

SCIENCE @ DIRECT®

Journal of Non-Crystalline Solids 316 (2003) 393–397

 JOURNAL OF
 NON-CRYSTALLINE SOLIDS

www.elsevier.com/locate/jnoncrysol

Letter to the Editor

Upconversion properties of a transparent Er^{3+} – Yb^{3+} co-doped LaF_3 – SiO_2 glass-ceramics prepared by sol–gel method

A. Biswas^{*}, G.S. Maciel¹, C.S. Friend, P.N. Prasad*Institute for Laser, Photonics and Biophotonics, NSM Complex, State University of New York, Buffalo, NY 14265, USA*

Received 4 December 2001; received in revised form 17 October 2002

Abstract

Transparent 0.1ErF_3 – 0.1YbF_3 – 5LaF_3 – 94.8SiO_2 (mol%) glass-ceramics was prepared by sol–gel method. Efficient upconversion emissions at 379, 407, 450, 490, 520, 540 and 660 nm were observed under 973 nm excitation. The signal at 379 nm is only ~ 4.5 times weaker than the signal at 520 nm, that is readily visible by the naked eyes even with a pump power of ~ 27 mW, indicating that this sample is a very good infrared-to-ultraviolet upconverter. The data obtained from transmission electron microscopy and X-ray diffraction studies indicate that the rare-earth ions were partitioned in the low phonon energy LaF_3 nanocrystals embedded in silica glass. The analysis of the dynamics of the upconversion emissions from level $^4\text{S}_{3/2}$ (~ 540 nm) and level $^4\text{F}_{9/2}$ (~ 660 nm) of Er^{3+} suggest that distinct energy transfer excitation pathways are responsible for populating these luminescent levels.

© 2003 Elsevier Science B.V. All rights reserved.

Rare-earth doped fluoride glasses are highly desirable materials for optical amplification [1,2], upconversion lasers [3] and display devices [4]. However, poor chemical and mechanical properties and low laser damage threshold make them unsuitable for practical use [5]. Silica based glasses, on the other hand, show excellent durability and optical quality. Unfortunately, large phonon energy of these oxide glasses increases the non-

radiative decay rate that reduces the luminescence efficiency [6,7].

Recently a new class of transparent glass-ceramics known as oxyfluoride glasses attracted much attention in which rare-earth doped fluoride nanocrystallites are dispersed in an oxide network [8]. The optical properties of the rare-earth ions in oxyfluoride glasses depend on the fluoride host while the mechanical properties of the glasses depend predominantly on the oxide host. Wang and Ohwaki [9] first reported ErF_3 – YbF_3 doped transparent oxyfluoride glass. They found that the green upconversion emission from oxyfluoride glass is 10 times brighter than that observed from fluoride glass. Kawamoto et al. [10] and Chen et al. [11] also reported strong upconversion emission from Er^{3+} doped oxyfluoride glass-ceramics.

^{*} Corresponding author. Present address: Center for High Technology Materials, 1313 Goddard SE, Albuquerque, NM 87106, USA. Tel.: +1-505 272 7093; fax: +1-505 272 7801.

E-mail address: abiswas@chtm.unm.edu (A. Biswas).¹ Present address: Departamento de Física, Universidade Federal Pernambuco, 50670-901 Recife, PE, Brazil.

Transparent LaF_3 glass-ceramics doped with rare-earth ions was found to be the most important class of oxyfluoride glasses [12]. Rare-earth doped lanthanum halide powders prepared by a sol-gel method coupled with HF reaction atmosphere were found to be highly efficient emitter at $1.3 \mu\text{m}$ [13]. In this letter we report optical properties of Er^{3+} in transparent $\text{LaF}_3\text{-SiO}_2$ ceramics prepared by a sol-gel method. We show that the infrared-to-ultraviolet upconversion efficiency is very high, indicating the potential of this material as a UV laser source for optical data storage and compact disk industry.

The glass-ceramics with composition of $0.1\text{ErF}_3\text{-}0.1\text{YbF}_3\text{-}5\text{LaF}_3\text{-}94.8\text{SiO}_2$ (mol%) were prepared using acid hydrolysis of tetraethylorthosilicate (TEOS). Fluorination was carried out in situ similar to that has been reported by Fujihara et al. [14]. In brief, TEOS, diluted with equal volume of ethyl alcohol was hydrolyzed with water. Acetic acid was used as catalyst. The molar ratio of $\text{TEOS:H}_2\text{O:CH}_3\text{COOH}$ was 1:10:0.5. The metal ions were used as their acetate salts. Separately, required amounts of dopant salts were dissolved completely in CF_3COOH so that the molar ratio of M^{3+} (where $\text{M} = \text{Er}^{3+}$, Yb^{3+} and La^{3+}) to F^- ions was 1:10. A small amount of water was used to speed up the dissolving process [14]. Finally, the salts solution was slowly mixed with TEOS sol with stirring and a homogeneous clear mixture was obtained. The resultant clear sol was then poured into petri dishes and covered with plastic sheets and allowed to form gels at room temperature. The gels were aged for 2 weeks at room temperature and finally dried in steps at different temperatures ($40\text{--}70^\circ\text{C}$) for 1 week in a temperature-controlled oven. The dried gels, which were slightly translucent in nature, were then heat-treated to 1000°C in air with different heating rate and allowed to furnace cool using a programmable temperature controller. The heating rate and soaking time at 1000°C were the most important parameters to obtain clear glass-ceramics. A faster heating rate and soaking time exceeding 5 min failed to yield clear sample. The samples densified with a heating rate of 75°C/h without any soaking at 1000°C were transparent. Fig. 1 shows the picture of a representative sample densified at

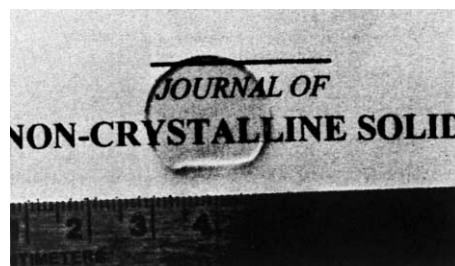


Fig. 1. Photograph of a glass-ceramics sample densified at 1000°C .

1000°C . The linear optical absorption (LOA) spectra of the polished samples were recorded with a spectrophotometer. The excitation source used to generate upconverted luminescence was an unfocused 800 mW single mode diode laser emitting at the near-infrared (973 nm). The UV-VIS fluorescence signals were recorded on a spectrofluorophotometer while the near-infrared fluorescence was measured using a monochromator coupled with an InGaAs detector. All the measurements were performed at room temperature.

The sample structural analysis was studied with transmission electron microscopy (TEM) and X-ray diffraction (XRD).

The LOA spectrum of the sample in the wavelength range of $250\text{--}1800 \text{ nm}$ is shown in Fig. 2. The absorption peaks are characteristic of $4f\text{--}4f$ electronic transitions of Er^{3+} and Yb^{3+} ions, being similar to that have been reported for Er^{3+} ions in

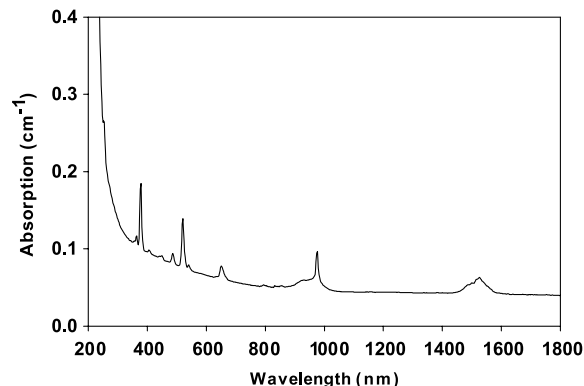


Fig. 2. Optical absorption spectrum of the glass-ceramics sample co-doped with Yb^{3+} (0.1 mol%) and Er^{3+} (0.1 mol%).

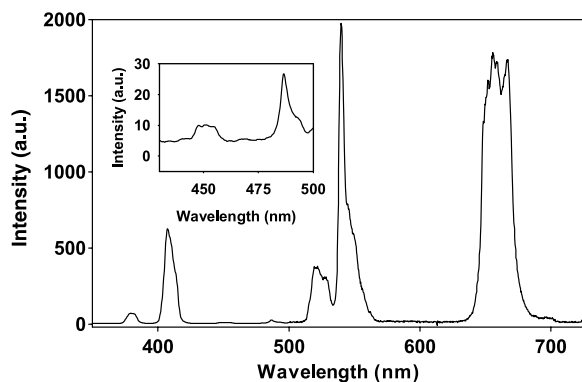


Fig. 3. Upconversion spectrum of the glass-ceramics excited with 973 nm laser diode (inset: magnified spectrum in the wavelength range of 430–500 nm).

oxyfluoride and other host materials [2,11]. Fig. 3 shows the upconversion spectrum of the sample in the wavelength range of 350–700 nm. Several peaks in the UV and VIS region have been observed correspond to transition of Er^{3+} ions from excited states to the ground state [15]. The peaks at 379, 407, 450, 489, 520, 540 and 660 nm are due to transitions ${}^4\text{G}_{11/2} \rightarrow {}^4\text{I}_{15/2}$, ${}^2\text{H}_{9/2} \rightarrow {}^4\text{I}_{15/2}$, ${}^4\text{F}_{5/2} \rightarrow {}^4\text{I}_{15/2}$, ${}^4\text{F}_{7/2} \rightarrow {}^4\text{I}_{15/2}$, ${}^2\text{H}_{11/2} \rightarrow {}^4\text{I}_{15/2}$, ${}^4\text{S}_{3/2} \rightarrow {}^4\text{I}_{15/2}$, and ${}^4\text{F}_{9/2} \rightarrow {}^4\text{I}_{15/2}$, respectively. The green emission peaked at 540 nm is very strong, being easily detected with naked eye even with ~ 27 mW of pump power. Note that the signal at 407 nm is the same order of magnitude as the signal at 520 nm. This was also observed in $\text{SiO}_2\text{-AlO}_{1.5}\text{-PbF}_2\text{-CdF}_2$ glass-ceramic doped with Yb^{3+} and Er^{3+} [11]. The intensity of the signal at 379 nm, on the other hand, is much more stronger in our glass-ceramic, with our intensity ratio $[520 \text{ nm}]/[379 \text{ nm}] \sim 4.5$, while for the sample of Ref. [11], this ratio is larger than 10^3 .

Upconversion emission from $\text{Er}^{3+}/\text{Yb}^{3+}$ co-doped matrix under 973 nm excitation is due to the resonant energy transfer from Yb^{3+} to Er^{3+} ions [16]. The multi-phonon relaxation rate of upconverted emissions is very sensitive to the phonon energy of the host matrix [17] and, thus, efficient upconversion is observed primarily in matrices with phonon of low cut-off energy (below 1000 cm^{-1}). The emissions from ${}^4\text{F}_J$ states, i.e. the bands at 450 and 490 nm, are hardly observed in

high-phonon energy matrices. The energy gap to the next lower levels from these ${}^4\text{F}_J$ levels is in the range $1000\text{--}1500 \text{ cm}^{-1}$. Therefore, de-excitation via multi-phonon relaxation to lower energy state is very likely to occur even in some non-oxide glasses. The presence of emission from ${}^4\text{F}_J$ levels in the present glass-ceramics is remarkable and indicates that the Er^{3+} ions are present in a local environment of very low phonon energy. LaF_3 has a cut-off phonon energy of 350 cm^{-1} compared to 1100 cm^{-1} of silica and therefore the Er^{3+} and Yb^{3+} ions in the glass-ceramics of study are expected to be confined in LaF_3 nanocrystallites rather than in a silica environment. Fig. 4 shows the TEM image of our glass-ceramics. The clusters of LaF_3 with average size of 10–20 nm are clearly visible as black spots. Electron diffraction pattern taken from one of these clusters indicates that these are crystalline in nature. This result is further supported by the XRD spectrum of the densified sample shown in Fig. 5. A broad diffraction pattern characteristic of the silica glass superimposed with sharp lines is observed. The diffraction peaks match with hexagonal LaF_3 , similar to that which was observed by others [12].

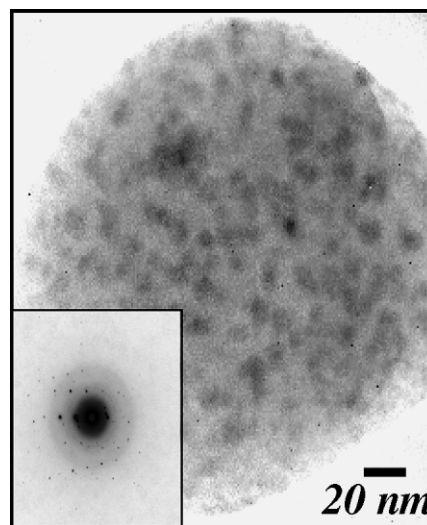


Fig. 4. TEM picture of the sample showing crystalline precipitates. The inset shows the electron diffraction pattern obtained from the precipitated region.

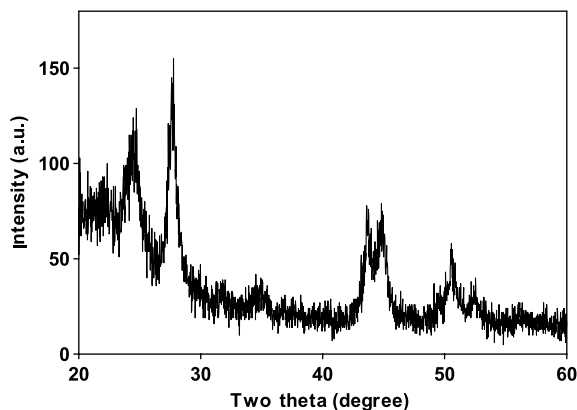


Fig. 5. XRD pattern of the glass-ceramics samples.

To measure the temporal characteristics of the stronger upconverted signals (green and red) the laser beam was chopped and the fluorescence dynamics was monitored with a time resolution better than 0.5 ms. The resolution was obtained by the decay time of the scattered light from the laser. The rise and decay times were obtained using single exponential fit of the data using standard commercial software. The rise and decay times of green (~540 nm) and red (~660 nm) lines are given in Table 1. As can be seen from the table, the decay time for the green line was limited by the resolution of the instrument. However, it is clear that both rise and decay times are longer for red than green line, which indicate different pathways of these emissions. There are basically two different channels to populate $^4S_{3/2}$ level: (a) Resonant energy transfer processes from a pair of excited Yb^{3+} ions to Er^{3+} : $^2F_{5/2}(Yb^{3+}) + ^2F_{5/2}(Yb^{3+}) + ^4I_{15/2}(Er^{3+}) \rightarrow ^2F_{7/2}(Yb^{3+}) + ^2F_{7/2}(Yb^{3+}) + ^4F_{7/2}(Er^{3+})$. Green emission is obtained when the excited Er^{3+} ions relax from state $^4F_{7/2}$ to $^4S_{3/2}$. (b) Energy transfer from an excited Yb^{3+} ion to Er^{3+} (populated at level $^4I_{11/2}$) followed by energy transfer between

two excited neighboring Er^{3+} ions at level $^4I_{11/2}$ in which the acceptor ion is excited to $^4F_{7/2}$ level while the donor de-excited to $^4I_{15/2}$. The excited state absorption is less probable than $Yb^{3+}-Er^{3+}$ energy transfer channel. This is because the ground state absorption of Yb^{3+} is larger than that of Er^{3+} and high doping level of Er^{3+} favors energy transfer between the neighboring atoms [18]. In our sample the molar concentration ratio of $Yb^{3+}:Er^{3+}$ ions is 1:1. Thus we believe that the second channel is more likely than the first channel, where the optimum ratio should be 2:1. In the case of phosphate glasses, significant energy transfer from Yb^{3+} to Er^{3+} ions was detected at the concentration ratio of 1:1 [19]. However, to get a better insight a concentration study is necessary (i.e. varying Yb^{3+} concentration while keeping the Er^{3+} concentration fixed) which is beyond the scope of the present work. For the red fluorescence, there are basically two channels of excitation as well. (a) Relaxation of population from level $^4S_{3/2}$ to level $^4F_{9/2}$; and (b) energy transfer upconversion via $^2F_{5/2}(Yb^{3+}) + ^4I_{13/2}(Er^{3+}) \rightarrow ^2F_{7/2}(Yb^{3+}) + ^4F_{9/2}(Er^{3+})$. Table 1 shows that the decay time of population at $^4S_{3/2}$ is short ($\leq 540 \mu s$) and therefore the decay rate $^4S_{3/2} \rightarrow ^4F_{9/2}$ must be that fast. This cannot explain the longer rise time of population at level $^4F_{9/2}$ (see Table 1). Therefore, the most likely channel of populating level $^4F_{9/2}$ should be through energy transfer from excited Yb^{3+} to excited Er^{3+} after relaxation from level $^4I_{11/2}$ to level $^4I_{13/2}$ takes place. This is reasonable because the lifetime of level $^4I_{11/2}$ is of a few milliseconds [20] and therefore the population loading at $^4F_{9/2}$ must be slower compared to that of level $^4S_{3/2}$.

Emission at 1300 nm due to $^1G_4 \rightarrow ^3H_5$ transition of Pr^{3+} has been reported in oxyfluoride glass [21] and it was argued that these glasses could replace ZBLAN in optical communication. Infrared downconversion emission was also observed in our sample. The fluorescence spectrum is shown in Fig. 6. in the wavelength range of 1400–1700 nm. The spectrum shows a broad emission with a peak at 1528 nm similar to that has been observed previously in oxyfluoride host, and it represents the $^4I_{13/2} \rightarrow ^4I_{15/2}$ transition. The full width at half maximum of the 1.5 μm emission band is 54 nm, which is significantly larger than that observed in

Table 1
Rise and decay times of the emission lines

Emission wavelength (nm)	Rise time (ms)	Decay time (ms)
540	2.30 ± 0.03	0.54 ± 0.03
660	3.20 ± 0.01	1.28 ± 0.00

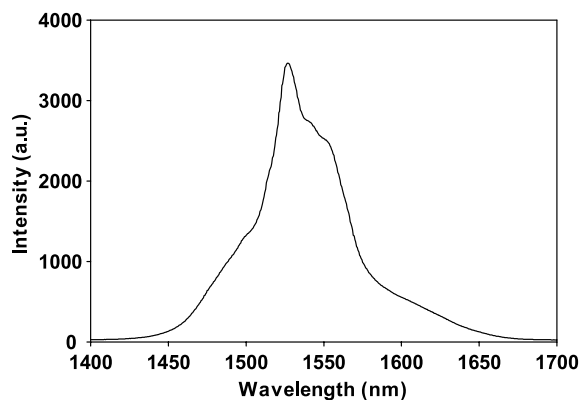


Fig. 6. Near-infrared luminescence spectrum of the glass-ceramics excited by a laser diode at 973 nm.

Er–silica glasses [22,23]. The spectrum is very similar to that has been reported for $\text{Er}^{3+}:\text{LaF}_3$ nano-particles [24] but is different from that observed in LaF_3 bulk or thin film [25]. This can be explained by the fact that the emission of Er^{3+} ions in present glass-ceramics is a combination of the emissions from the ions at or near the surface that is significantly influenced by SiO_2 matrix and the ions in the core of the LaF_3 nano-particles. The broadband emission spectrum is due to the distorted crystal field on Er^{3+} ions caused by large size mismatch between La^{3+} and Er^{3+} ions [8]. This broadband emission is very important in designing tunable IR amplifiers for optical communications.

In conclusion, a transparent $0.1\text{ErF}_3-0.1\text{YbF}_3-5\text{LaF}_3-94.8\text{SiO}_2$ (mol%) glass-ceramics has been developed by the sol–gel method. Er^{3+} ions are coupled with low phonon energy in a nano-crystalline LaF_3 matrix that led to efficient infrared-to-ultraviolet upconversion.

References

- [1] Y. Ohishi, T. Kanamori, T. Kitagawa, S. Takahashi, E. Snitzer, G.H. Sigel, *Opt. Lett.* 16 (1991) 1747.
- [2] G.S. Maciel, N. Rakov, C.B. de Araujo, Y. Messaddeq, J. *Opt. Soc. Am. B* 16 (1999) 1995.
- [3] J.F. Massicott, M.C. Brierley, R. Wyatt, S.T. Davey, D. Szebesta, *Electron. Lett.* 29 (1993) 2119.
- [4] E. Downing, L. Hesselink, J. Ralston, R. Macfarlane, *Science* 273 (1996) 1185.
- [5] P.N. Kumta, S.H. Risbud, *J. Mater. Sci.* 29 (1991) 135.
- [6] T. Miyakawa, D.L. Dexter, *Phys. Rev. B* 1 (1970) 2961.
- [7] R.S. Quimby, M.G. Drexhage, M.J. Suscavage, *Electron. Lett.* 23 (1987) 32.
- [8] M.J. Dejneka, *MRS Bull.* 11 (1998) 57.
- [9] Y. Wang, J. Ohwaki, *Appl. Phys. Lett.* 63 (1993) 3268.
- [10] Y. Kawamoto, R. Kanno, J. Qiu, *J. Mater. Sci.* 33 (1998) 63.
- [11] X.B. Chen, Y.X. Ni, W.M. Du, N. Sawanobori, *Opt. Commun.* 184 (2000) 289.
- [12] M.J. Dejneka, *J. Non-Cryst. Solids* 239 (1998) 149.
- [13] J. Ballato, R.E. Riman, E. Snitzer, *Opt. Lett.* 22 (1997) 691.
- [14] S. Fujihara, C. Mochizuki, T. Kimura, *J. Non-Cryst. Solids* 244 (1999) 267.
- [15] M.J. Weber, *Phys. Rev.* 157 (1967) 262.
- [16] F. Auzel, *Proc. IEEE* 61 (1993) 758.
- [17] L. Wetenkamp, G.F. West, H. Többen, *J. Non-Cryst. Solids* 140 (1992) 35.
- [18] P.S. Golding, S.D. Jackson, T.A. King, M. Pollnau, *Phys. Rev. B* 62 (2000) 856.
- [19] B.-C. Hwang, S. Jiang, T. Luo, J. Watson, G. Sorbello, N. Peyghambarian, *J. Opt. Soc. Am. B* 17 (2000) 833.
- [20] S. Bedö, M. Pollnau, W. Lüthy, H.P. Weber, *Opt. Commun.* 116 (1995) 81.
- [21] P.A. Tick, N.F. Borrelli, L.K. Cornelius, M.A. Newhouse, *J. Appl. Phys.* 78 (1995) 6367.
- [22] B.T. Stone, K.L. Bray, *J. Non-Cryst. Solids* 197 (1996) 136.
- [23] A. Biswas, H.N. Acharya, *Indian J. Pure Appl. Phys.* 35 (1997) 532.
- [24] J.W. Stouwdam, F.C.J.M. van Veggel, *Nano Lett.* 2 (2002) 733.
- [25] C. Buchal, T. Siegrist, D.C. Jacobson, J.M. Poate, *Appl. Phys. Lett.* 68 (1996) 438.